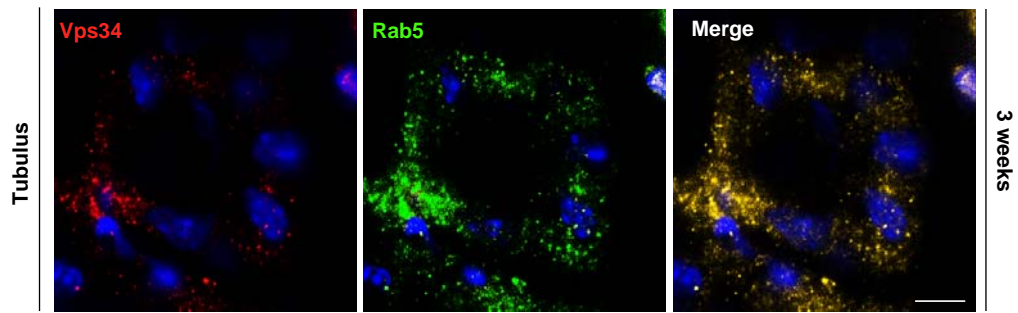
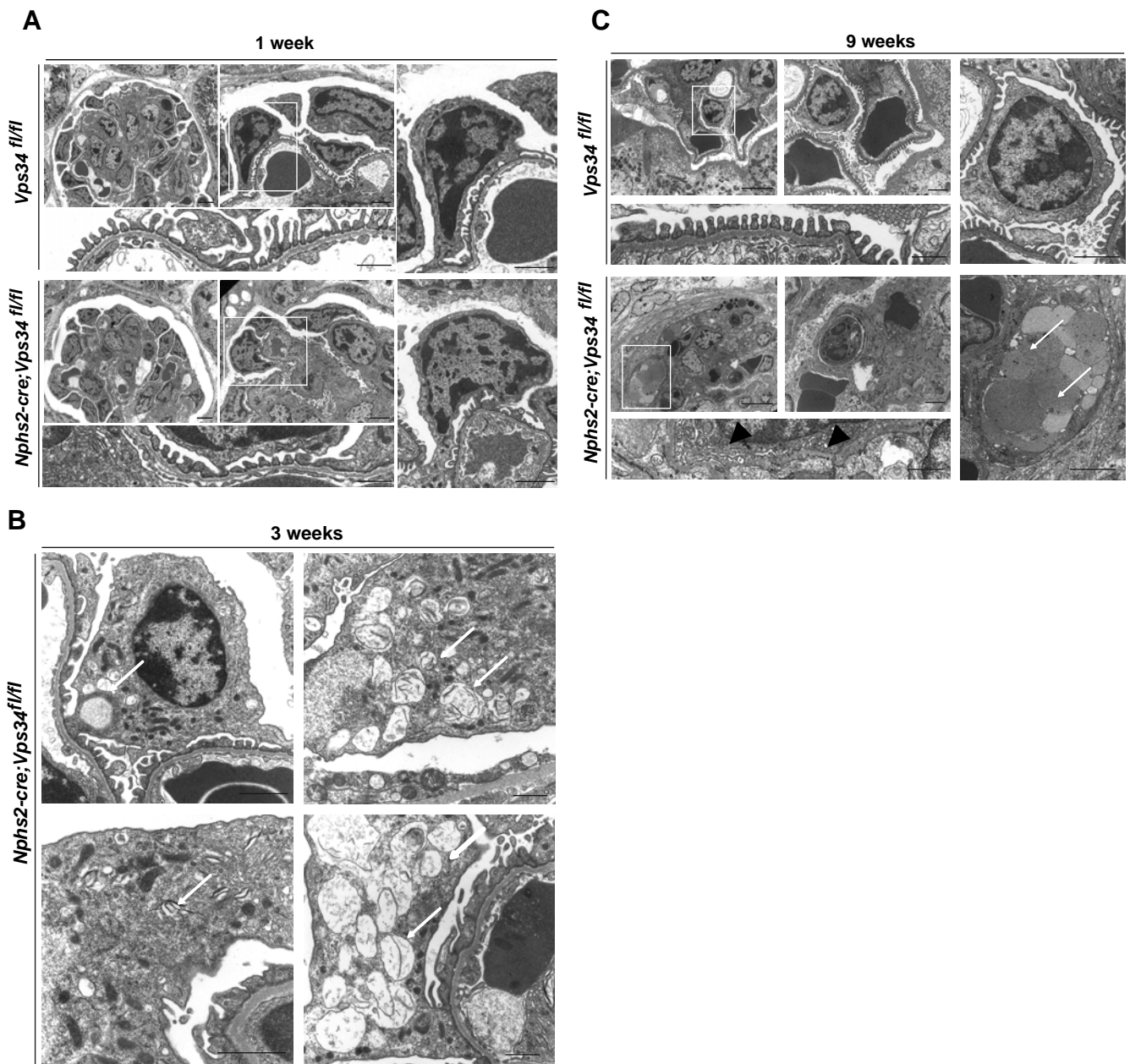


## Figure Supplementary 1



**Figure S1. Tubular Rab5 expression and co-localisation with Vps34.** Co-labelling immunofluorescence stainings with Rab5 and Vps34 on mouse kidney sections.

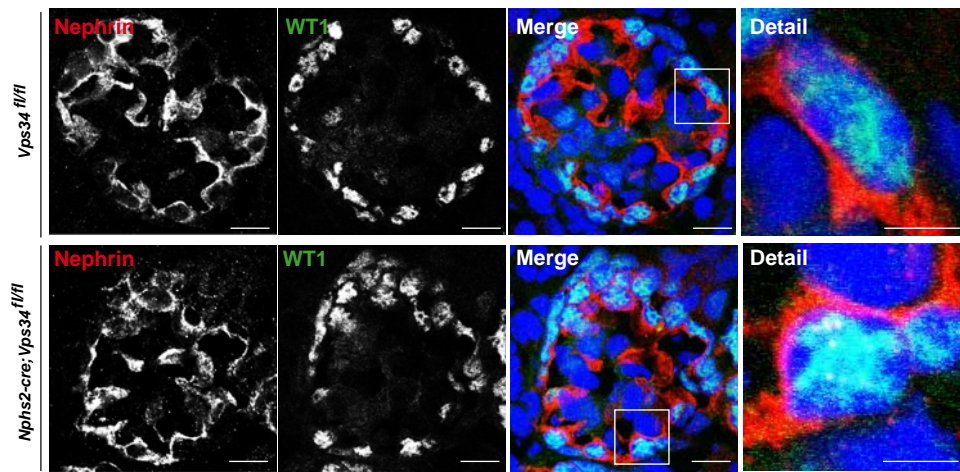
## Supplementary Figure 2



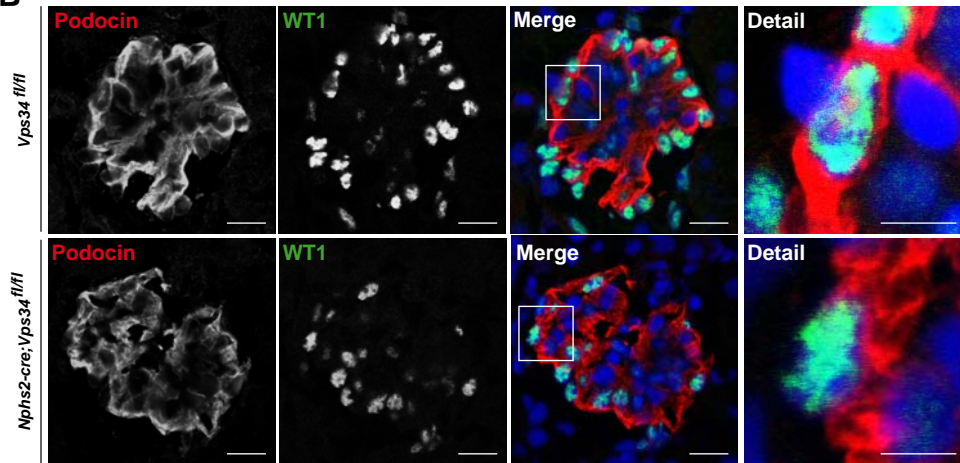
**Figure S2. Podocyte specific Vps34 deficiency causes massive vacuolization and rapid podocyte degeneration.** (A) Electron microscopy of kidney sections of 1 week old mice. Glomerular overview of *Nphs2-cre;Vps34<sup>fl/fl</sup>* and littermate controls (left upper panels) displayed no significant differences in podocyte morphology. Podocytes (right panels) and slit diaphragm (lower panels) show only marginal early signs of foot process effacement in 1 week old *Nphs2-cre;Vps34<sup>fl/fl</sup>* kidney sections compared to littermate control sections. Scale bars 5  $\mu$ m (upper left panels), 2  $\mu$ m (upper middle panels), 1  $\mu$ m (right panels) and 500nm lower panels. (B) Electron microscopy of kidney sections of 3 weeks old mice showed single-membrane, large-sized vacuoles in *Vps34* deficient podocytes (arrows). Scale bars 1  $\mu$ m for upper left panel, 500nm for upper and lower right panel, 200nm for lower left panel. (C) Electron microscopy of kidney sections of 9 weeks old *Nphs2-cre;Vps34<sup>fl/fl</sup>* mice showed substantial vacuolization of podocytes (white arrows), complete loss of foot processes (black arrow heads) and severe glomerulosclerosis compared to littermate control mice. Scale bars 5  $\mu$ m (upper left panels), 2  $\mu$ m (upper middle panels), 1  $\mu$ m (right panels) and 500nm lower panels.

## Supplementary Figure 3

**A**



**B**



**C**

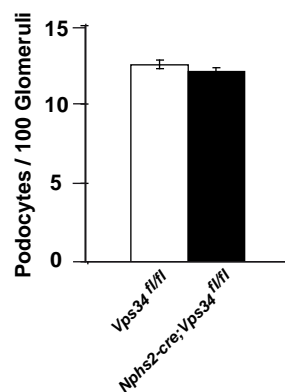


**Figure S3. Staining for slit diaphragm proteins and the podocyte marker WT1 displayed no significant difference in *Nphs2-cre;Vps34fl/fl* mice compared to littermate control mice at 1 week of age.** (A, B) Immunofluorescence stainings of kidney sections of *Nphs2-cre;Vps34fl/fl* and littermate controls for the slit diaphragm proteins Nephlin and Podocin and the podocyte nucleus marker WT1 demonstrated equal distribution of slit diaphragm proteins and no difference in podocyte cell numbers in *Nphs2;Vps34fl/fl* mice and littermate controls 1 week after birth. Scale bars 10µm; 5µm for details. (C) Podocyte cell quantification at 1 week of age. Podocyte numbers were estimated by counting the number of WT1-positive cells per glomerular cross-section in 100 randomly selected glomeruli / kidney. No differences in the number of podocytes / glomerulus were detected in kidneys of *Nphs2-cre;Vps34fl/fl* mice or littermate controls ( $P = 0.84$ , 2-tailed Student's  $t$  test,  $n = 3$  mice for each condition).



## Supplementary Figure 4

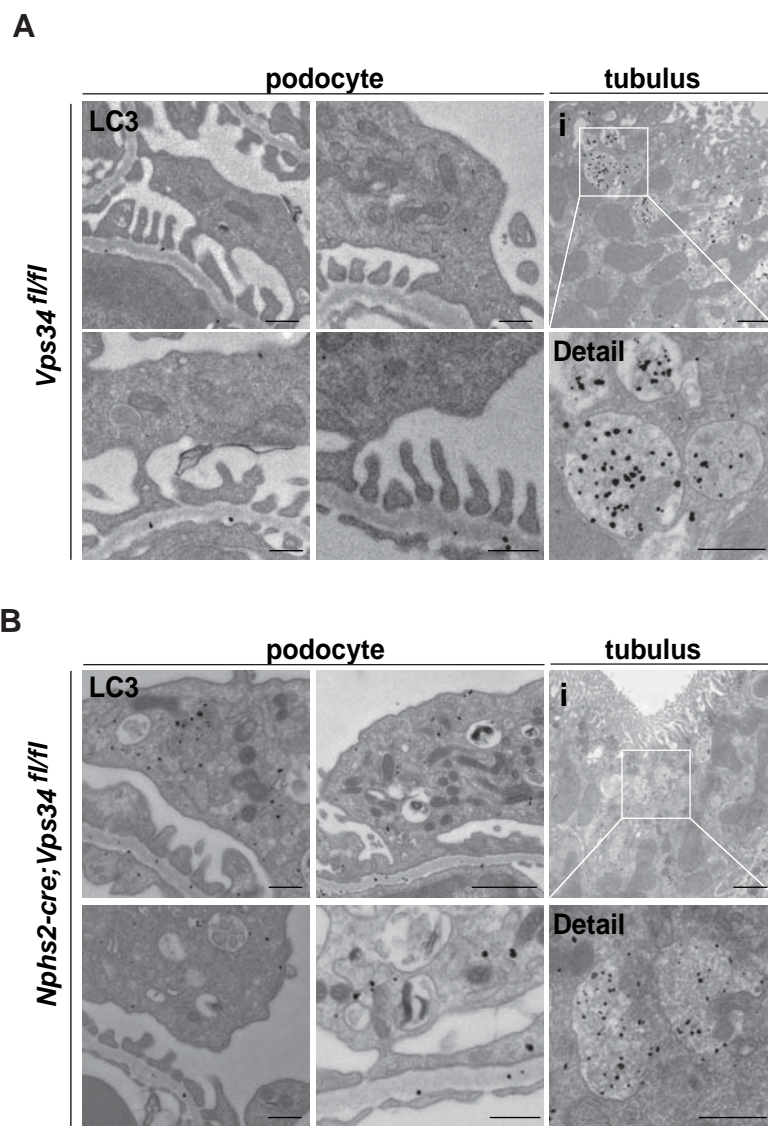


**Figure S4. Immunogold electron microscopy analysis.** Fixed kidney sections of 3-weeks-old *Nphs2-cre;Vps34<sup>fl/fl</sup>* mice and control littermates were incubated overnight with anti-LC3 and with a 1.4-nm gold-coupled goat anti-mouse secondary antibody for immunogold reaction and further processed for electron microscopy. (A) Wildtype podocytes display only very few LC3 gold particles. Representative sections of tubular cells (i), rich in autophagosomes confirm the specific localization of LC3-gold particles to autophagosomes. Scale bars: 500nm. (B) In *Vps34*-deficient podocytes, gold particles aggregate diffusely in the cytoplasm but do not co-localize with autophagosomal membranes. Gold particle deposition to the basal membrane is equal in wildtype and *Nphs2-cre;Vps34<sup>fl/fl</sup>* renal sections and most likely unspecific due to immunocomplex deposits and / or negative electric charge of the basal membrane. Representative sections of tubular cells (i), rich in autophagosomes confirm the specific localization of LC3-gold particles to autophagosomes. Scale bars: 500nm.

## Supplementary Figure 5

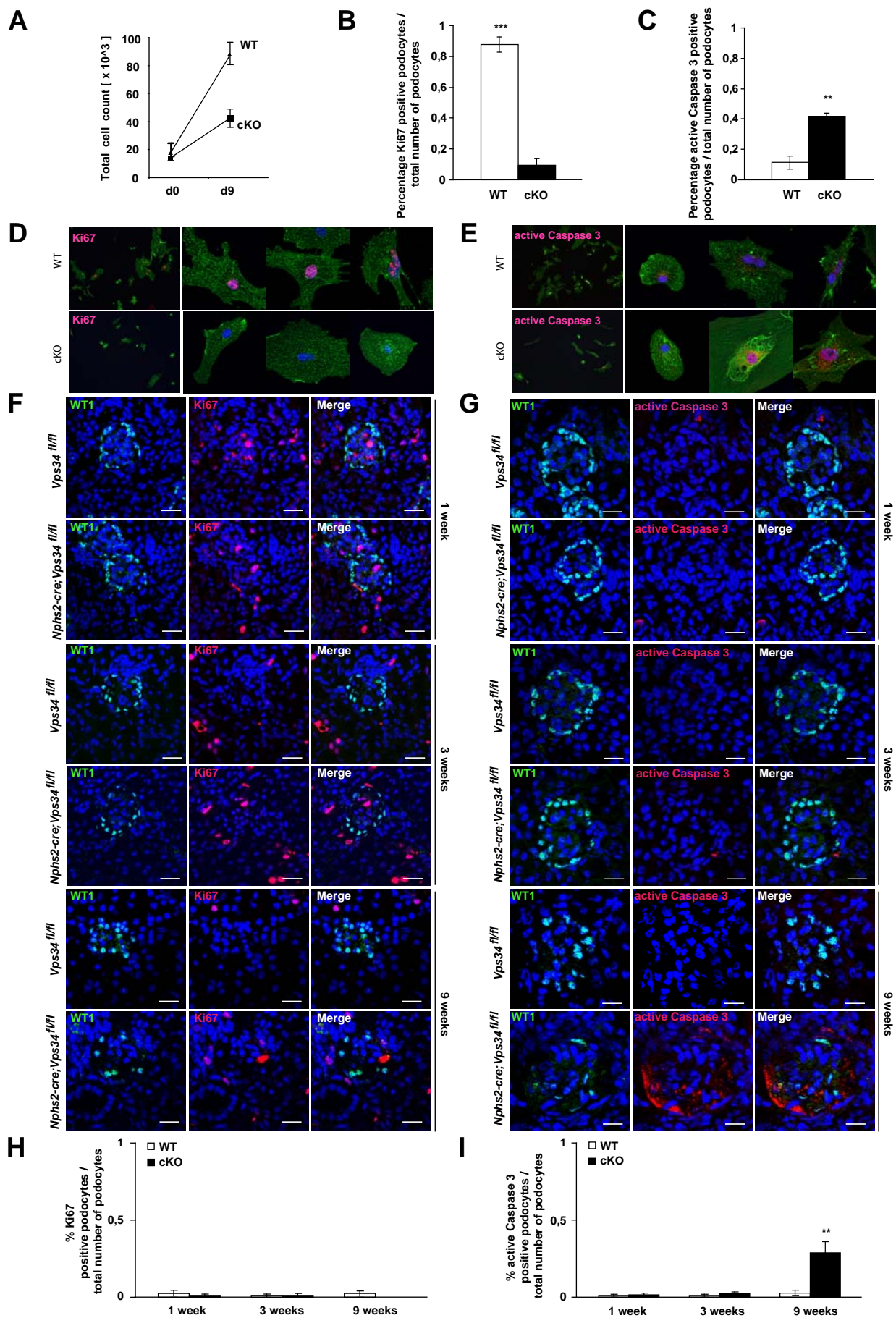
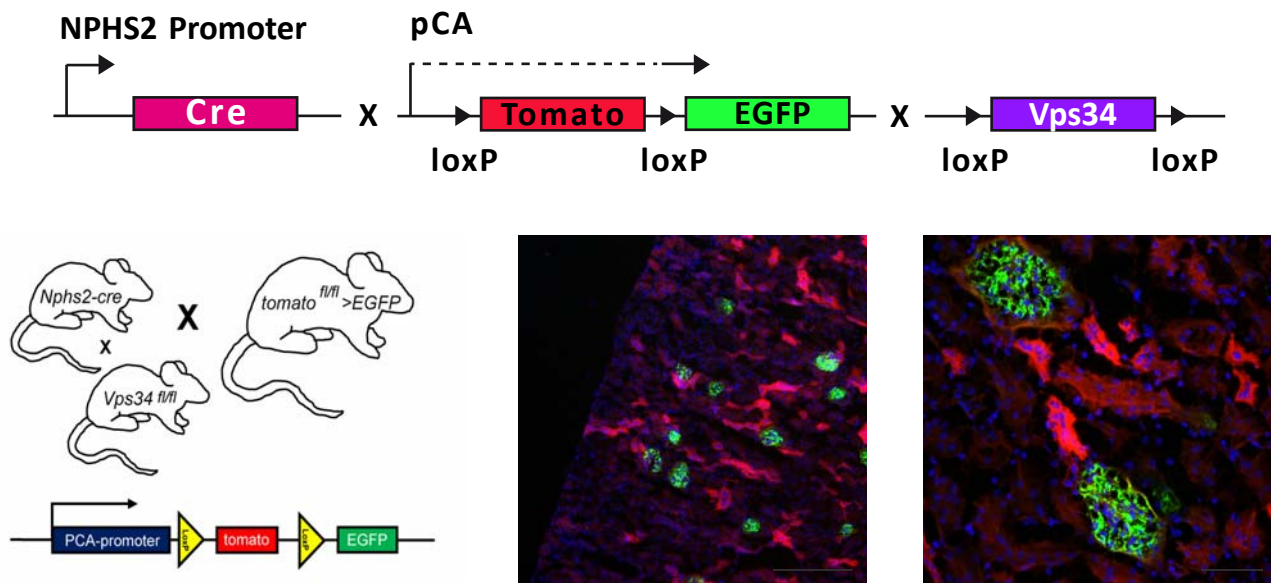


**Figure S5. Primary podocytes isolated from *Nphs2-cre;Vps34<sup>fl/fl</sup>;tomatofl/+>EGFP* mice exhibited strongly reduced proliferation compared to wildtype controls.** (A) Significant reduction in the total cell count of Vps34-deficient primary podocytes after 9 days compared to GFP-positive control podocytes. (B-E) Quantification and immunofluorescence stainings of primary podocytes isolated from conditionally Vps34-deficient mice and littermate controls. (B, D) Primary wildtype podocytes show enhanced proliferation (illustrated by Ki-67 staining) whereas Vps34-deficient podocytes did not. (C, E) Active caspase 3 staining revealed that, in vitro, primary Vps34-deficient podocytes die, at least in part, from apoptosis. (F, G) Immunofluorescence stainings and quantification of kidney sections of conditionally Vps34-deficient mice and littermate controls. (F) In vivo, Ki-67 staining showed no significant proliferation activity of neither WT nor Vps34-deficient podocytes at different time points. Podocytes were co-stained with WT1. (G) Active caspase 3 staining of kidney sections showed increased apoptosis in 9 weeks old mice in parietal cells, mesangial cells and podocytes. At early stages of beginning glomerulosclerosis (week 3), active caspase 3 staining was indifferent from WT podocytes.

## Supplementary Figure 6

A



B

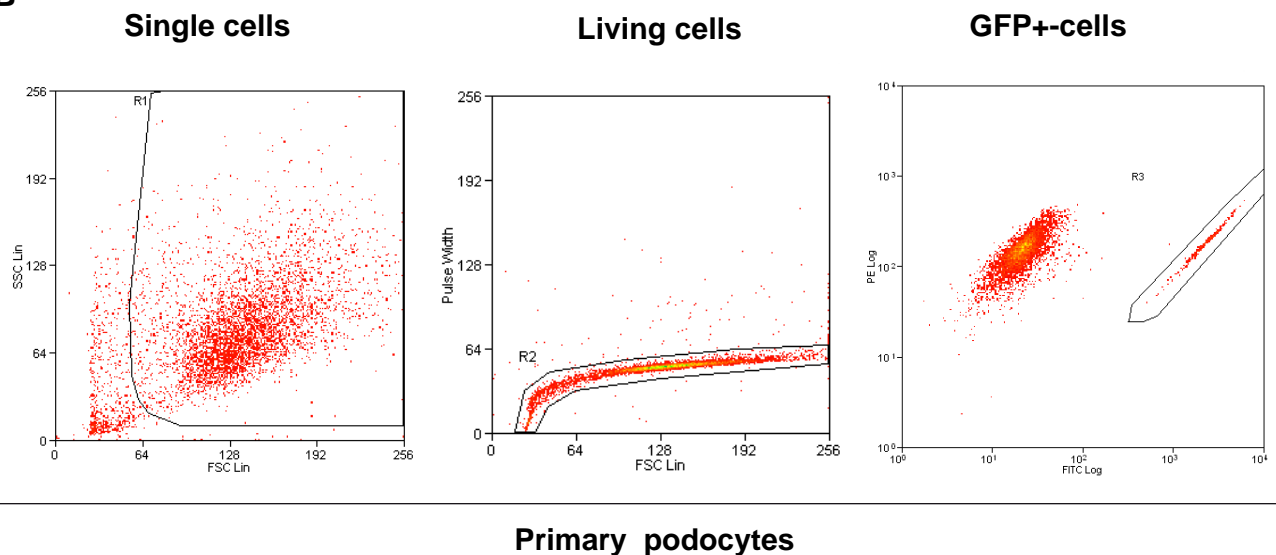


**Figure S6. FACS sorting of GFP-positive primary podocytes.** (A) On postnatal day 10, glomeruli from Nphs2-cre;Vps34<sup>fl/fl</sup>;tomato<sup>fl/+</sup>>EGFP mice and littermate controls were isolated by a sieving protocol, established in our lab and cultured for several days. (B) After podocytes had grown out of the glomeruli, cells were trypsinated and GFP-positive cells were FACS sorted and maintained in primary cell culture medium. Representative flow cytometric data, regions and sort gate.